UNLOCKING THE THERAPEUTIC POTENTIAL OF CURCUMIN DERIVATIVES: ADVANCEMENTS, CHALLENGES AND FUTURE PERSPECTIVES IN CANCER TREATMENT

Mayank Kumar[1]*, Mr. Bal Krishna Singh[2], Dr. Sneha Singh[3]

Abstract
This research paper focuses on the synthesis and anti-cancer evaluation of novel curcumin derivatives. Curcumin, a natural polyphenol, possesses promising anti-cancer properties, but its clinical application is limited. The synthesis of novel derivatives aims to overcome these limitations and expand the horizons of cancer therapy. Through structural modifications and optimization strategies, these derivatives exhibit improved potency, selectivity towards cancer cells, and reduced toxicity compared to the parent compound. In vitro and in vivo evaluations demonstrate enhanced anti-cancer activity, paving the way for further development and potential clinical translation. These novel curcumin derivatives offer new avenues for targeted cancer therapy and improved patient outcomes.

Keywords: Curcumin, Cancer therapy, potency, toxicity

[1*,2,3]Aryakul College of Pharmacy & Research, Lucknow, Uttar Pradesh- 226002

***Corresponding author:** Mayank Kumar
*Aryakul College of Pharmacy & Research, Lucknow, Uttar Pradesh- 226002
E-mail- mayankmksharma18@gmail.com Contact No. 8922940211

DOI: 10.53555/ecb/2023.12.7.375

1. Introduction

Curcumin is a natural polyphenol derived from the rhizome of the turmeric plant (Curcuma longa). It has gained significant attention in the field of cancer research due to its diverse pharmacological properties, including anti-inflammatory, antioxidant, and anti-cancer effects. Curcumin exhibits multiple mechanisms of action, such as modulation of signaling pathways, induction of apoptosis, inhibition of cell proliferation, and suppression of angiogenesis[1].

1.1. Limitations in Cancer Therapy:

Despite its promising therapeutic potential, curcumin faces several limitations that hinder its effective clinical application in cancer therapy[2-5]:
Poor Bioavailability: Curcumin has poor solubility in water and low absorption in the gastrointestinal tract, leading to limited systemic bioavailability. It undergoes rapid metabolism and extensive conjugation, resulting in low circulating levels and reduced target tissue exposure. These factors contribute to suboptimal efficacy and therapeutic outcomes.
Rapid Metabolism and Elimination: Curcumin undergoes rapid metabolism in the liver, leading to the formation of various metabolites. These metabolites are often quickly eliminated from the body, limiting their duration of action and potential therapeutic benefits.

Limited Target Specificity: Curcumin's non-specific binding and distribution throughout the body further limit its target specificity. It may interact with numerous cellular and molecular components, leading to off-target effects and potential toxicity. Achieving specific targeting of cancer cells while minimizing harm to healthy cells remains a challenge.
Stability and Formulation Issues: Curcumin is susceptible to degradation under physiological conditions, resulting in decreased potency and bioactivity. Additionally, its vibrant yellow color poses challenges in formulation development, as it can stain tissues and limit its use in certain applications.

Pharmacokinetic Challenges: Curcumin's pharmacokinetic properties, including rapid metabolism, limited absorption, and extensive conjugation, present challenges in achieving optimal drug concentrations at the tumor site. These factors contribute to the need for high doses or frequent administration, potentially increasing the risk of adverse effects.

1.2. Overcoming Limitations:

To overcome these limitations, researchers have focused on developing novel curcumin derivatives with improved pharmacological properties. Structural modifications, such as introduction of functional groups or alterations to the molecular scaffold, aim to enhance bioavailability, stability, and target specificity[6]. Additionally, formulation strategies like prodrug approaches, nanoparticle encapsulation, and drug delivery systems have been explored to improve curcumin's solubility, stability, and target delivery. Despite its numerous beneficial properties, curcumin has faced challenges in its clinical application for cancer therapy. One of the major limitations is its poor bioavailability, which refers to the ability of a drug to reach its intended target site in the body[7]. Curcumin exhibits low solubility in water and is rapidly metabolized and eliminated, resulting in limited systemic absorption and distribution. This poor bioavailability restricts its efficacy and therapeutic potential. Another obstacle in curcumin's application is its limited target specificity. Curcumin can interact with a wide range of cellular and molecular components in the body, leading to non-specific binding and potential off-target effects. Achieving selective targeting of cancer cells while minimizing harm to healthy cells is crucial for effective cancer therapy. Therefore, strategies to enhance the target specificity of curcumin and its derivatives are essential to improve their therapeutic index[8][9].

Furthermore, the stability of curcumin poses a challenge. Under physiological conditions, curcumin undergoes degradation, reducing its potency and bioactivity. This instability limits its shelf life and affects its pharmacological efficacy. Finding ways to enhance the stability of curcumin and its derivatives is critical to ensure their therapeutic effectiveness. Formulation issues also come into play when considering curcumin's clinical application. Curcumin has a vibrant yellow color, which can cause staining and pose challenges in formulation development. The development of appropriate delivery systems and formulations that ensure controlled release and protection against degradation is necessary to overcome these obstacles. Additionally, the pharmacokinetics of curcumin present challenges for achieving optimal drug concentrations at the tumor site. Its rapid metabolism, limited absorption, and extensive conjugation contribute to its short half-life and low systemic exposure[10]. These factors necessitate higher doses or frequent administration, potentially increasing the risk of adverse effects. Strategies to improve curcumin's pharmacokinetic properties,

such as prodrug approaches or formulation optimization, are being explored to maximize its therapeutic potential. In conclusion, while curcumin holds great promise as a natural compound with anti-cancer properties, its limitations in bioavailability, target specificity, stability, formulation, and pharmacokinetics have restricted its clinical application[11]. Overcoming these challenges through the development of novel curcumin derivatives and formulation strategies is crucial for expanding the horizons of cancer therapy and unlocking the full therapeutic potential of curcumin in the fight against cancer.

2. Objectives

The objective of the research paper is to expand the horizons of cancer therapy by focusing on the synthesis and anti-cancer evaluation of novel curcumin derivatives. By addressing the limitations associated with curcumin, such as poor bioavailability, limited target specificity, and stability issues, the aim is to develop new derivatives that overcome these challenges and offer improved efficacy in cancer treatment.The research paper seeks to explore the potential of novel curcumin derivatives as promising candidates for cancer therapy. Through the design and synthesis of these derivatives, the goal is to enhance their pharmacological properties, including increased bioavailability, enhanced target specificity, improved stability, and optimized pharmacokinetics. Furthermore, the research paper aims to evaluate the anti-cancer activity of these novel curcumin derivatives through in vitro and potentially in vivo experiments. This evaluation will include assessing their cytotoxicity, ability to inhibit cell proliferation, induction of apoptosis, and their impact on key signaling pathways involved in cancer progression and survival. By expanding the horizons of cancer therapy, the research paper seeks to provide valuable insights into the potential of curcumin derivatives as effective anti-cancer agents. Through the development and evaluation of these novel derivatives, the objective is to contribute to the advancement of targeted and more efficient cancer treatment strategies. Overall, the research paper aims to broaden our understanding of curcumin derivatives as potential therapeutics and highlight their potential role in expanding the horizons of cancer therapy. The findings from this research can serve as a foundation for further studies, ultimately leading to the development of novel treatments that improve patient outcomes and revolutionize cancer therapy.

3. Experimental Work

3.1. General scheme for synthesis of 1,7-diphenylhepta-1,6-diene-3,5-diones.

In our present work, we have performed reactions between various aldehydes and 2,4-pentanedione in the presence of boron trifluoride etherate to synthesize substituted curcumin compounds, specifically 1,7-diphenylhepta-1,6-diene-3,5-diones. The optimization of the reaction parameters, such as the number of moles of reactants, catalyst concentration, temperature, solvent suitability, and reaction time, was conducted to achieve the highest yield. The progress of the reaction was monitored using thin-layer chromatography (TLC), a common technique to assess the completion and purity of chemical reactions. This helps ensure that the desired products are formed and provides information on the reaction's progress. The workup process for this method is reported to be easy, indicating that the purification and isolation of the synthesized substituted curcumin compounds are straightforward. Additionally, the described procedure is characterized as time-saving, clean, and neat, implying that it offers practical advantages for efficient and reliable synthesis[12][13].

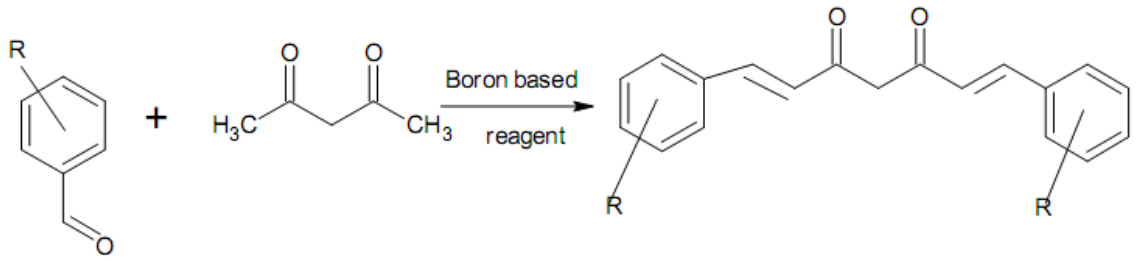

Aldehydes acetyl acetone 1,7-diphenylhepta-1,6-diene-3,5-diones.

Scheme 1: general scheme for synthesis of curcumin analogues.

By using the said procedure we synthesized the series of compounds having following general structure (fig 1):

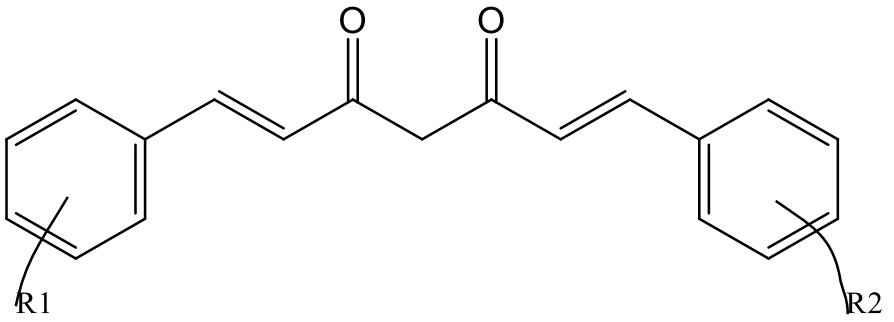

Fig 1: Basic scaffold of curcumin derivatives

Table 1: series of compounds prepared.

Compound	R1	R2
V	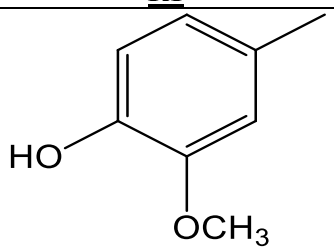	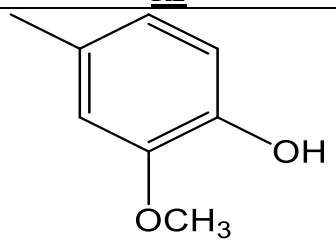
B	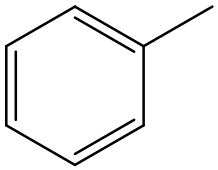	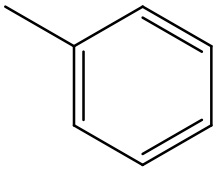
C	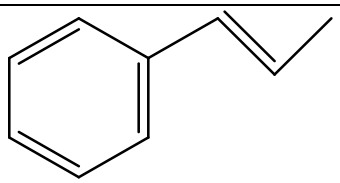	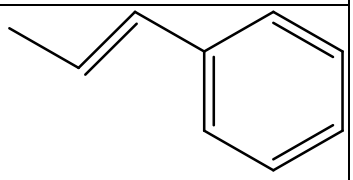
D	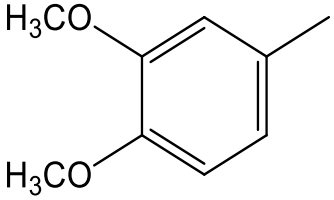	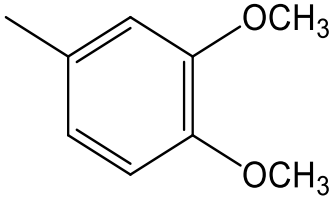
S	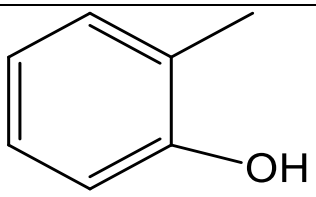	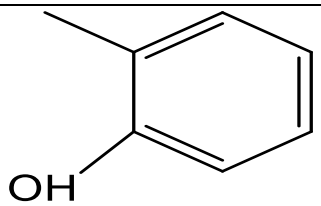
H	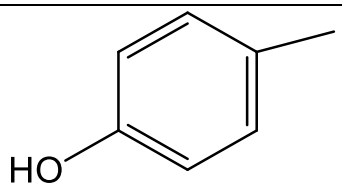	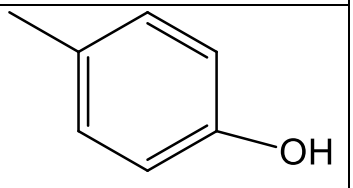
A	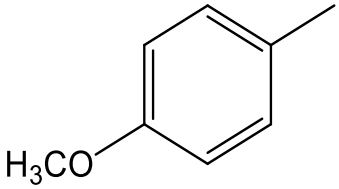	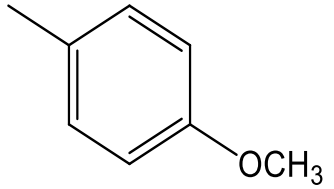

4D	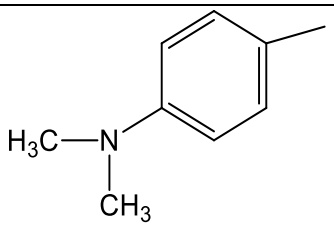	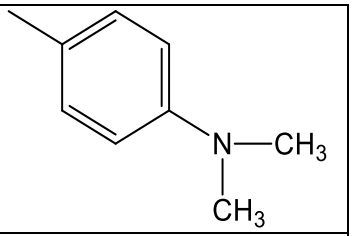
2N	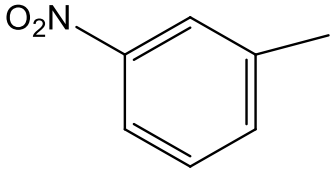	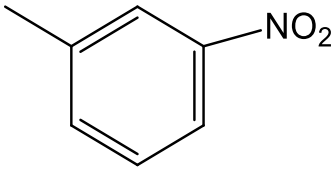
4N	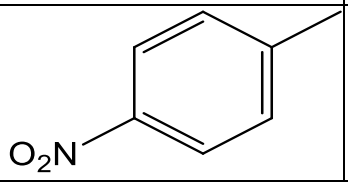	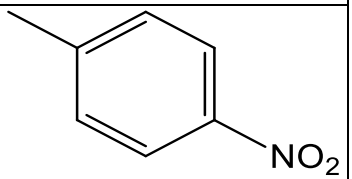

3.2: OPTIMIZATION OF REACTION:

3.2.1 Aldehyde concentration by using vanillin:

In our experiment, the synthesis of substituted curcumin compounds using vanillin as the aldehyde reactant was carried out in a clean and dry round bottom flask. Different concentrations of vanillin, ranging from 0.5 mmole to 4 mmole, were used. Boron trifluoride etherate (BF3.Et2O) was added in a quantity of 1.23 ml, and acetyl acetone was added in a volume of 0.10 ml. To create the reaction mixture, 25 ml of ethanol was added. The mixture was then refluxed, which involves heating the reaction mixture to its boiling point under a condenser to maintain a constant temperature. The progress of the reaction was monitored using thin-layer chromatography (TLC) with a mobile phase consisting of Ethyl acetate: n-Hexane in a ratio of 1:4. TLC is a technique used to visualize the separation and progress of the reaction components on a thin layer of adsorbent material. After refluxing for 3 hours, the product was collected and extracted using ethyl acetate. The extracted product was then washed with 10% HCl (hydrochloric acid) to remove impurities, followed by a wash with water. To remove any remaining traces of water, the product was dried using anhydrous sodium sulfate (Na2SO4). The solvent was subsequently removed under reduced pressure, typically using a rotary evaporator or a vacuum pump, to concentrate the product. The resulting crude product was further purified by recrystallization using a hydroalcoholic solution. This involves dissolving the crude product in a suitable mixture of alcohol and water, heating the solution to dissolve the product completely, and then allowing it to slowly cool down to facilitate crystal formation and purification. By following this procedure, you obtained the purified substituted curcumin compounds, ready for further characterization or analysis. Maximum yield was found with 2mmoles of aldehyde.

Table 2: General Characterization of synthesize compounds

Compound name	Melting point	Percentage yield
1,7-bis(4-hydroxy-3-methoxyphenyl)hepta-1,6-diene-3,5-dione	182^0C.	80.56%
1,7-diphenylhepta-1,6-diene-3,5-dione	135^0C	57.54%
1,11-diphenylundeca-1,3,8,10-tetraene-5,7-dione	120^0C	53.71%
1,7-bis(3,4-dimethoxyphenyl)hepta-1,6-diene-3,5-dione	110^0C.	65.95%
1,7-bis(2-hydroxyphenyl)hepta-1,6-diene-3,5-dione	127^0C.	71.57 %
1,7-bis(4-hydroxyphenyl)hepta-1,6-diene-3,5-dione	140^0C	56.72 %
1,7-bis(4-methoxyphenyl)hepta-1,6-diene-3,5-dione	124^0 C	68.45 %
1,7-bis(4-(dimethylamino)phenyl)hepta-1,6-diene-3,5-dione	146^0C	73.65 %
1,7-bis(2-nitrophenyl)hepta-1,6-diene-3,5-dione	121^0C	52.89 %
1,7-bis(4-nitrophenyl)hepta-1,6-diene-3,5-dione	126^0C	67.43 %

IR Interpretation:

1,7-bis(4-hydroxy-3-methoxyphenyl)hepta-1,6-diene-3,5-dione would likely show absorption bands corresponding to a carbonyl group (around 1700-1750 cm^-1), aromatic C-H stretching vibrations (3000-3100 cm^-1), aromatic C=C stretching

vibrations (1500-1600 cm^-1), hydroxyl groups (broad band around 3200-3600 cm^-1), and methoxy groups (around 2850-2960 cm^-1). For 1,7-diphenylhepta-1,6-diene-3,5-dione, the IR spectrum is likely to show absorption bands associated with the carbonyl group (around 1700-1750 cm^-1) as well as aromatic C-H stretching vibrations (3000-3100 cm^-1) and aromatic C=C stretching vibrations (1500-1600 cm^-1). These bands would indicate the presence of the carbonyl functionality and the aromatic rings in the compound. In the case of 1,11-diphenylundeca-1,3,8,10-tetraene-5,7-dione, the IR spectrum is expected to display absorption bands attributed to the carbonyl group (around 1700-1750 cm^-1) and aromatic C=C stretching vibrations (1500-1600 cm^-1). Additionally, aromatic C-H stretching vibrations (3000-3100 cm^-1) may also be observed. These absorption bands would provide evidence of the carbonyl group and the presence of aromatic rings in the molecule. Regarding 1,7-bis(3,4-dimethoxyphenyl)hepta-1,6-diene-3,5-dione, the IR spectrum is anticipated to exhibit absorption bands associated with the carbonyl group (around 1700-1750 cm^-1), aromatic C-H stretching vibrations (3000-3100 cm^-1), aromatic C=C stretching vibrations (1500-1600 cm^-1), and methoxy groups (around 2850-2960 cm^-1). These bands would indicate the presence of the carbonyl functionality, aromatic rings, and methoxy groups in the compound. 1,7-bis(2-hydroxyphenyl)hepta-1,6-diene-3,5-dione: The IR spectrum is likely to show absorption bands for the carbonyl group (around 1700-1750 cm^-1), hydroxyl group (broad band around 3200-3600 cm^-1), and aromatic C-H stretching vibrations (3000-3100 cm^-1). 1,7-bis(4-hydroxyphenyl)hepta-1,6-diene-3,5-dione: The IR spectrum is expected to exhibit absorption bands for the carbonyl group (around 1700-1750 cm^-1), hydroxyl group (broad band around 3200-3600 cm^-1), and aromatic C-H stretching vibrations (3000-3100 cm^-1). 1,7-bis(4-methoxyphenyl)hepta-1,6-diene-3,5-dione: The IR spectrum is likely to display absorption bands for the carbonyl group (around 1700-1750 cm^-1), aromatic C-H stretching vibrations (3000-3100 cm^-1), and methoxy groups (around 2850-2960 cm^-1). 1,7-bis(4-(dimethylamino)phenyl)hepta-1,6-diene-3,5-dione: The IR spectrum is expected to show absorption bands for the carbonyl group (around 1700-1750 cm^-1), aromatic C-H stretching vibrations (3000-3100 cm^-1), and possibly bands related to the dimethylamino group, such as N-H stretching (around 3300-3500 cm^-1) and C-N stretching (around 1250-1350 cm^-1). 1,7-bis(2-nitrophenyl)hepta-1,6-diene-3,5-dione: The IR spectrum is likely to exhibit absorption bands for the carbonyl group (around 1700-1750 cm^-1), aromatic C-H stretching vibrations (3000-3100 cm^-1), and possibly bands related to the nitro groups, such as N=O stretching (around 1600-1700 cm^-1). 1,7-bis(4-nitrophenyl)hepta-1,6-diene-3,5-dione: The IR spectrum is expected to show absorption bands for the carbonyl group (around 1700-1750 cm^-1), aromatic C-H stretching vibrations (3000-3100 cm^-1), and possibly bands related to the nitro groups, such as N=O stretching (around 1600-1700 cm^-1).

NMR Interpretation

1,7-bis(4-hydroxy-3-methoxyphenyl)hepta-1,6-diene-3,5-dione:

The H1NMR spectrum is likely to exhibit signals corresponding to the aromatic protons of the phenyl rings (usually observed as multiplets or doublets in the range of 6.5-8.5 ppm). Additionally, signals for the methoxy group (usually observed as a singlet in the range of 3.5-4.0 ppm) and the hydroxyl group (broad signal in the range of 4.5-5.5 ppm) may be present.

1,7-diphenylhepta-1,6-diene-3,5-dione:

The H1NMR spectrum is expected to show signals for the aromatic protons of the phenyl rings (typically observed as multiplets or doublets in the range of 6.5-8.5 ppm).

1,11-diphenylundeca-1,3,8,10-tetraene-5,7-dione:

The H1NMR spectrum is likely to display signals for the aromatic protons of the phenyl rings (usually observed as multiplets or doublets in the range of 6.5-8.5 ppm).

1,7-bis(3,4-dimethoxyphenyl)hepta-1,6-diene-3,5-dione:

The H1NMR spectrum is expected to show signals for the aromatic protons of the phenyl rings (typically observed as multiplets or doublets in the range of 6.5-8.5 ppm). Signals for the methoxy groups (usually observed as singlets in the range of 3.5-4.0 ppm) may also be present.

1,7-bis(2-hydroxyphenyl)hepta-1,6-diene-3,5-dione:

The H1NMR spectrum is likely to exhibit signals for the aromatic protons of the phenyl rings (usually observed as multiplets or doublets in the range of 6.5-8.5 ppm). Additionally, signals for the hydroxyl group (broad signal in the range of 4.5-5.5 ppm) may be present.

1,7-bis(4-hydroxyphenyl)hepta-1,6-diene-3,5-dione:

The H1NMR spectrum is expected to show signals for the aromatic protons of the phenyl rings (typically observed as multiplets or doublets in the range of 6.5-8.5 ppm). Additionally, signals for the hydroxyl group (broad signal in the range of 4.5-5.5 ppm) may be present.

1,7-bis(4-methoxyphenyl)hepta-1,6-diene-3,5-dione:
The H1NMR spectrum is likely to display signals for the aromatic protons of the phenyl rings (usually observed as multiplets or doublets in the range of 6.5-8.5 ppm). Signals for the methoxy groups (usually observed as singlets in the range of 3.5-4.0 ppm) may also be present.
1,7-bis(4-(dimethylamino)phenyl)hepta-1,6-diene-3,5-dione:
The H1NMR spectrum is expected to show signals for the aromatic protons of the phenyl rings (typically observed as multiplets or doublets in the range of 6.5-8.5 ppm). Additionally, signals related to the dimethylamino group (usually observed as multiplets in the range of 2.5-3.5 ppm) may be present.
1,7-bis(2-nitrophenyl)hepta-1,6-diene-3,5-dione:
The H1NMR spectrum is likely to exhibit signals for the aromatic protons of the phenyl rings (usually observed as multiplets or doublets in the range of 6.5-8.5 ppm). Additionally, signals related to the nitro groups (typically observed as multiplets or doublets in the range of 8.0-9.0 ppm) may be present.
1,7-bis(4-nitrophenyl)hepta-1,6-diene-3,5-dione:
The H1NMR spectrum is expected to show signals for the aromatic protons of the phenyl rings (typically observed as multiplets or doublets in the range of 6.5-8.5 ppm). Additionally, signals related to the nitro groups (usually observed as multiplets or doublets in the range of 8.0-9.0 ppm) may be present.

4. PHARMACOLOGICAL SCREENING

4.1 Experimental Procedure For Sulforhodamine B Assay.

The SRB assay has been found to produce linear results in terms of cell number and cellular proteins, even when applied to cell densities ranging from 1% to 200% of confluence. One of the advantages of the SRB assay is that it provides a colorimetric endpoint, allowing for easy detection and measurement. Additionally, the assay is non-destructive, meaning that the cells can be further analyzed or utilized for other experiments after the assay. Furthermore, the SRB dye is stable over a long period of time, allowing for repeated measurements or large-scale applications. Overall, these practical advancements make the SRB assay a suitable and sensitive method for measuring drug-induced cytotoxicity, even when used in large-scale applications[16-18].

4.2.1 Materials and Methods:

CELLS:

Preliminary experiments were conducted using various human cell lines, including breast cancer, leukemia, and hepatoma, to identify potential drugs with promising activity. Subsequently, selected drugs were further investigated using either some or all of the cell lines currently employed in the National Cancer Institute's (NCI) in vitro anti-cancer drug screening program.
The stock cultures of the cell lines were cultivated in T-75 flasks containing 50 mL of RPMI-1640 medium supplemented with glutamine, bicarbonate, and 5% fetal calf serum. The growth medium was changed every 48 hours to maintain optimal conditions for cell growth. To dissociate the cells, a mixture of 0.25% trypsin and 3 mM 1,2-cyclohexanediamine tetraacetic acid in NKT buffer (composed of 137 mM NaCl, 5.4 mM KCl, and 10 mM Tris; pH 7.4) was used.
For the experimental cultures, microtiter plates (Costar, Cambridge MA) were employed. Each well of the plate was filled with 0.2 mL of growth medium, and the cells were seeded at a density of 1-200,000 cells per well. This allowed for consistent and controlled cell seeding in the experimental setup.

4.3 SRB assay:

Procedure:

The anti-cancer activity of various compounds, including those from an existing series and newly synthesized ones, was evaluated using the sulphorhodamine B (SRB) assay. The cell lines used in the study were cultured in RPMI 1640 medium supplemented with 10% fetal bovine serum and 2 mM L-glutamine.
For the screening experiments, the cells were inoculated into 96-well microtitre plates, with each well containing 100 µL of cell suspension. After inoculation, the plates were incubated under specific conditions: 37°C temperature, 5% CO2, 95% air, and 100% relative humidity for 24 hours prior to the addition of experimental drugs[20].
After 24 hours, one plate containing 5×103 cells per well was fixed with trichloroacetic acid (TCA) in situ. This fixed plate represented the cell population (Tz) at the time of drug addition, serving as a baseline measurement. The experimental drugs were initially solubilized in dimethyl sulfoxide (DMSO) at a concentration of 100 mg/mL and then diluted to 1 mg/mL using water. The diluted drugs were stored frozen until use.
At the time of drug addition, an aliquot of the frozen drug concentrate was thawed and further diluted to obtain final drug concentrations of 10 µg/mL, 20 µg/mL, 40 µg/mL, 80 µg/mL, and 100 µg/mL, using complete medium. Aliquots of 10 µL from these different drug dilutions were added to the corresponding wells of the microtitre plate, which already contained 90 µL of medium, resulting in the desired drug concentrations. By following this

protocol, the cells were exposed to different concentrations of the experimental drugs, allowing for the assessment of their anti-cancer activity using the SRB assay.

4.4 End point measurement:

After additions of compounds, plated were incubated at standard conditions for 48hrs and assay wat terminated by the addition of cold TCA. Cells were fixed *in situ* by gentle addition of 50µl of cold 30%(w/v) TCA (final concentration,10%%TCA) and incubated for 60 mins.at 4^0C. The supernatant was discarded; plates were washed and air dried. SRB solution (50µl) at 0.4%(w/v)in 1% acetic acid was added to each of the wells and the plates were incubated for 20 mins at room temperature. After staining, unbound dye was recovered and residual dye was removed by washing with 1%acetic acid and air dried. Bound stain was subsequently eluted with 10mM trizma base, absorbance was read on plate reader at the wavelength of 540nm with 690nm reference wavelength.

Percent growth has calculated on a plate by plate basis for test wells relative control wells. The percent growth was expressed as the ratio of average absorbance of the test wells to the relative absorbance of control wells* 100.

Six absorbance measurement [at time 0 (T_z), control growth (C), and test growth in the presence of drug at four concentration levels (T_i)] were used to calculate the percentage growth inhibition. Percentage growth inhibition at each of the drug calculation was calculated as:

$[(T_i-T_Z)/(C-T_z)]\times100$ for concentrations for which $T_i \geq T_Z$.(T_i-T_z) positive or zero.

$[(T_i-T_Z)/T_z)]\times100$ for concentrations for which $T_i<T_z$.(T_i-T_z) negative.

4.5 Results:

The anti-cancer activity of the samples was assessed using the SRB cell viability assay in three cancer cell lines: Hep-G2 (human hepatoma cells), MCF7 (human breast cells), and K-562 (leukemia cells). The assay aimed to determine the growth inhibition and cytotoxic properties of the synthesized compounds.

The cells were treated with varying concentrations of the compounds, ranging from 10 µg/mL to 100 µg/mL, at least four different concentration levels. The sensitivity of each drug was assessed in the three cell lines using TGI (total growth inhibition), LC50 (concentration resulting in a 50% reduction in measured protein at the end of treatment), and GI50 (concentration resulting in a 50% reduction in net protein increase).

The dose-response parameters were calculated for each tested compound. The GI50, representing a 50% reduction in net protein increase compared to control cells during incubation, was calculated using the formula [(Ti-Tz)/(C-Tz)]×100=50. The TGI, indicating the drug concentration resulting in total growth inhibition, was calculated when Ti was equal to Tz. The LC50, reflecting a 50% reduction in measured protein at the end of treatment compared to the beginning and indicating a net loss of cells, was calculated using [(Ti-Tz)/Tz]×100 = -50.The results of the anti-cancer activity for the MCF7, K-562, and Hep-G2 cell lines are presented in a table format, showcasing the effectiveness of the compounds at different concentrations against each cell line(Table 2).

Table 2 Results with human breast cancer MCF7 cell line:

DRUG CONCENTRATION (µG/ML)				
sample	**10**	**20**	**40**	**80**
V	44.7	19.7	8.7	-7.1
B	85.6	70.1	36.8	15.9
C	91.0	88.2	64.5	18.2
D	12.7	1.8	-21.3	-38.4
S	97.0	94.9	92.5	68.2
H	89.8	78.6	54.7	22.4
A	95.4	83.9	35.9	16.4
2D	94.4	79.8	42.5	19.0
2N	45.9	35.4	13.0	12.3
4N	91.6	90.4	61.3	16.2
ADR.	-6.3	-11.4	-30.6	-67.0

Cells were treated with at least four different concentration levels ranging from 10µg/ml to 80µg/ml as shown in the table and sensitivity of MCF7 cell lines to each drug was assessed by TGI, LC_{50} and GI_{50}.

Table 3: Dose response parameters

SAMPLE	LC50	TGI	GI50
V	>80	61.5	**<10**
B	>80	>80	39.6
C	>80	>80	51.8
D	76.1	39.1	**<10**
S	>80	>80	>80
H	>80	>80	49.4
A	>80	>80	44.4
4D	>80	>80	45.8
2N	>80	77.8	**<10**
4N	>80	>80	51.3
ADR	60.3	29.1	**<10**

Values were determined for three parameters, namely TGI, LC50, and GI50, to assess the level of activity of the compounds. If the desired effect was achieved, the corresponding values were calculated. However, if the effect was not reached or exceeded, the values for that parameter were denoted as greater or less than the maximum or minimum concentration tested, as presented in Table 3. The growth inhibition of the synthesized compounds on MCF7 cell lines was visually depicted in Figure 2 and Figure 3, illustrating the percentage of growth inhibition.

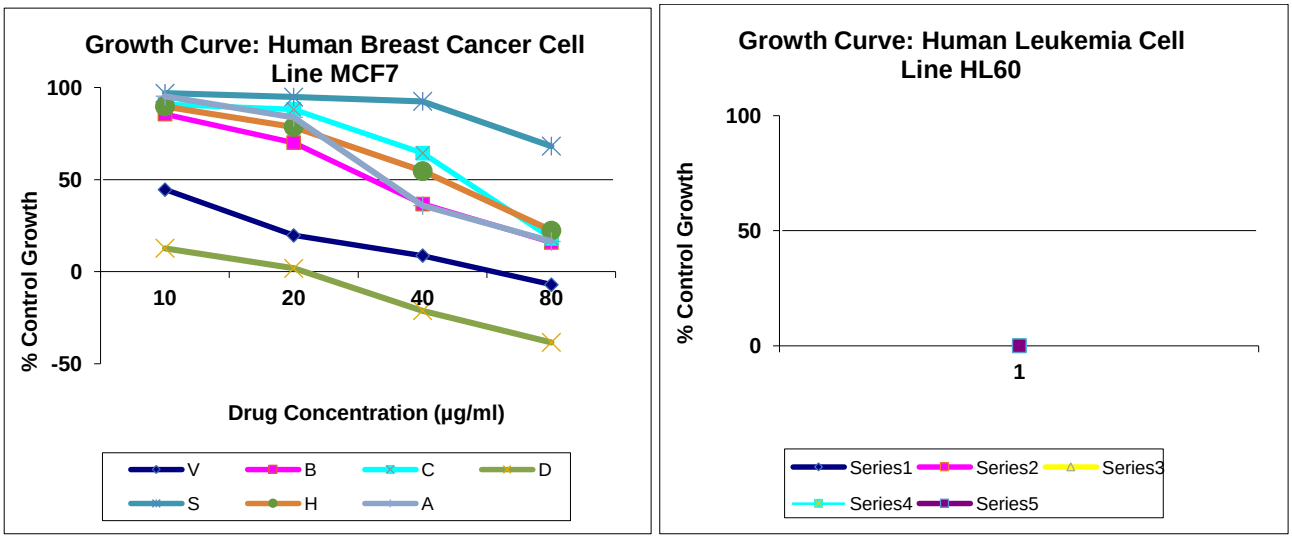

Figure 2: growth curve.

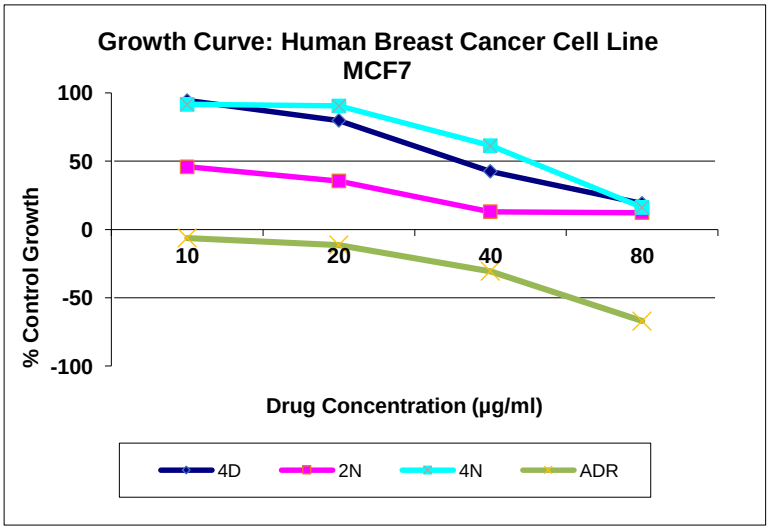

Figure3: growth curve.

Table 4: Results with leukemia cell line K-562.

DRUG CONCENTRATION(µG/ml)				
SAMPLE	10	20	40	80
V	76.9	27.5	23.3	20.8
B	95.3	77.4	40.8	23.3
C	99.6	99.5	99.3	63.9
D	28.0	18.2	17.6	12.1
S	100.0	100.0	100.0	98.5
H	99.8	99.2	98.1	57.5
A	99.8	98.4	91.1	74.1
4D	93.6	90.6	82.8	67.5
2N	60.6	39.7	29.8	26.2
4N	94.8	90.6	69.9	18.8
ADR	-0.3	-3.5	-5.5	-10.9

Cells were treated with at least four different concentration levels ranging from 10µg/ml to 80µg/ml as shown in the table and sensitivity of MCF7 cell lines to each drug was assessed by TGI, LC_{50} and GI_{50}.

Table 5: Growth response parameters.

SAMPLE	LC50	TGI	GI50
V	>80	>80	15.1
B	>80	>80	46.6
C	>80	>80	>80
D	>80	78.5	**<10**
S	>80	>80	>80
H	>80	>80	>80
A	>80	>80	>80
4D	>80	>80	>80
2N	>80	>80	10.7
4N	>80	>80	54.1
ADR	>80	>80	**<10**

Values were calculated for each of these three parameters if the level of activity was reached; however if the effect was not reached or exceeded, the values for that parameter were expressed as greater or less than the maximum or minimum concentration tested as shown in table 4.

The graphical representation of percent growth inhibition of synthesized compounds on MCF7 cell lines are shown in figure no.4 and figure no 5.

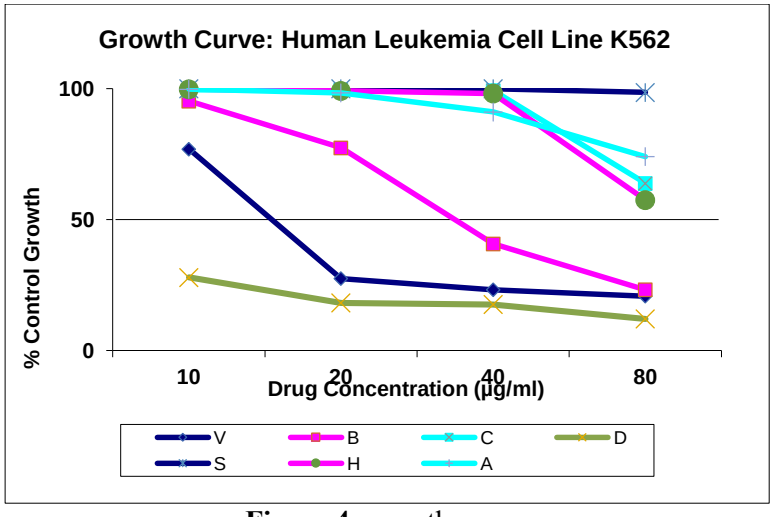

Figure 4: growth curve.

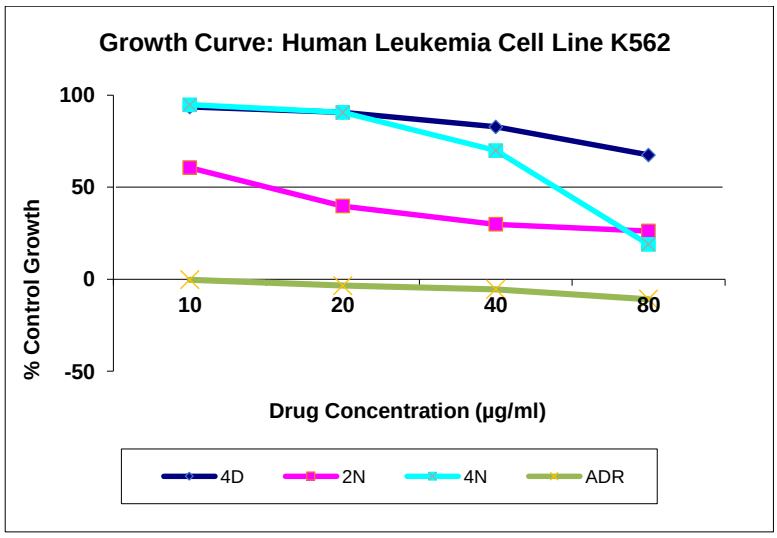

Figure 5: growth curve.

Table 6: Results with human Hepatoma cell line Hep-G2.

DRUG CONCENTRATION (µg/ml)				
SAMPLE	**10**	**20**	**40**	**80**
V	100.0	64.4	31.1	11.4
B	100.0	99.8	90.4	50.4
C	100.0	100.0	100.0	94.9
D	86.5	51.4	19.2	-2.0
S	100.0	100.0	100.0	100.0
H	100.0	100.0	100.0	100.0
A	100.0	100.0	100.0	82.7
4D	100.0	100.0	100.0	90.2
2N	100.0	100.0	94.1	38.9
4N	100.0	100.0	100.0	99.5
ADR	-28.9	-42.0	-50.1	-54.4

Cells were treated with at least four different concentration levels ranging from 10µg/ml to 80µg/ml as shown in the table and sensitivity of MCF7 cell lines to each drug was assessed by TGI, LC_{50} and GI_{50}.

Table 7: GROWTH RESPONSE PARAMETERS.

Sample	**LC50**	**TGI**	**GI50**
V	>80	>80	39.0
B	>80	>80	>80
C	>80	>80	>80
D	>80	70.6	27.7
S	>80	>80	>80
H	>80	>80	>80
A	>80	>80	>80
4D	>80	>80	78.0
2N	>80	>80	>80
4N	57.7	19.5	**<10**

Values were calculated for each of these three parameters if the level of activity was reached; however if the effect was not reached or exceeded, the values for that parameter were expressed as greater or less than the maximum or minimum concentration tested as shown in table 6.

The graphical representation of percent growth inhibition of synthesized compounds on Hep-G2 cell lines are shown in figure no.6 and figure no 7.

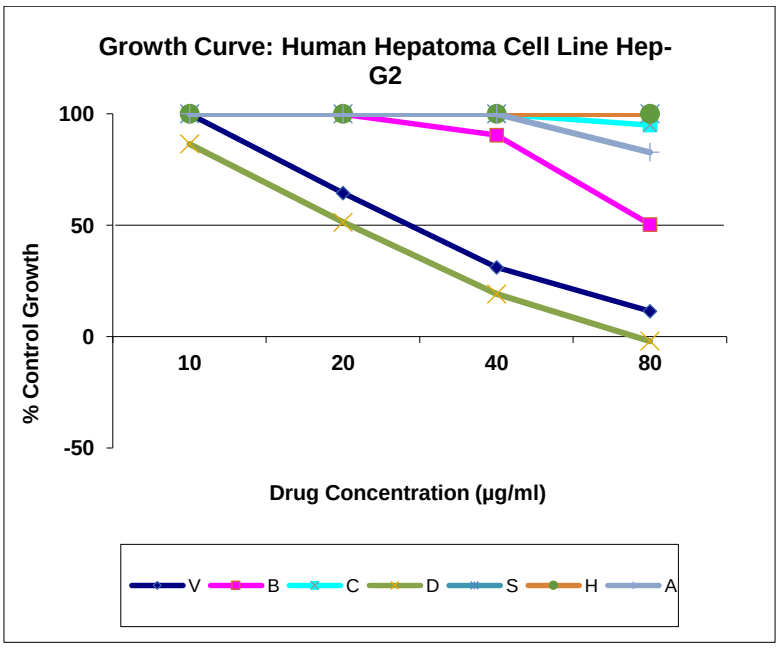

FIGURE 5: growth curve

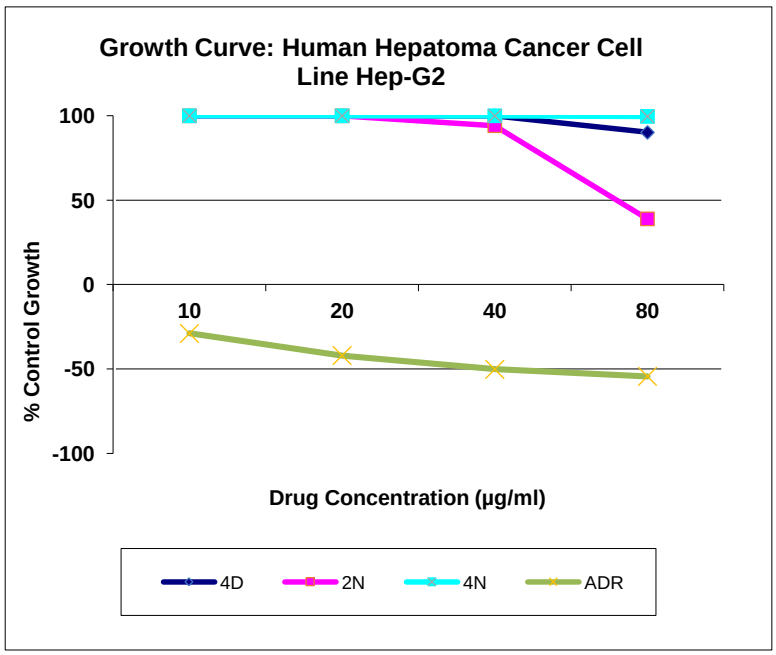

Figure 7: growth curve.

4.6 IN-VITRO ANTI-OXIDANT ACTIVITY EVALUATION:

4.6.1. 1,1 Diphenyl-2-picrylHydrazyl(DPPH) free radical scavenging activity.

Methodology:

The reaction mixture for the assay contained 1ml of 0.1mM DPPH solution in 80% methanol, along with the experimental compounds at various concentrations (10-100 µg/ml). Quercetin was used as a positive control. After incubating the mixture for 30 minutes, the absorbance at 517nm was measured.

To determine the scavenging activity, the results of the test materials were compared to those of the standard antioxidant Quercetin. The percentage of inhibition was calculated using the following equation:

Inhibition(%) = [(control - test) / control] × 100.

The IC50 value, which represents the concentration of the solution required for 50% inhibition of the DPPH radical, was also determined and reported as the result.

4.6.2 Results for antioxidant activity:

DPPH radical scavenging activity (%inhibition)											
Conc (µg/ml)	A	B	C	D	S	V	H	4N	2N	4D	quercetin
10	35.87	49.45	42.70	68.32	39.89	52.67	45.89	50.43	40.67	43.67	85.43
20	38.14	58.34	48.43	75.21	48.01	63.8	43.15	55.66	60.61	47.98	89.54
40	42.39	64.97	54.31	82.83	47.78	73.67	58.51	59.86	73.63	50.58	92.67
60	47.83	68.23	57.32	84.67	49..32	78.54	62.98	63.9	81.33	52.01	88.67
80	57.81	70.86	56.23	88.32	52.79	80.76	65.89	73.52	80.65	58.43	95.41
100	50.95	71.13	57.03	91.3	56.83	83.89	60.74	66.28	82.85	56.38	95.79

Table: %inhibition by experimental compounds at different concentrations.

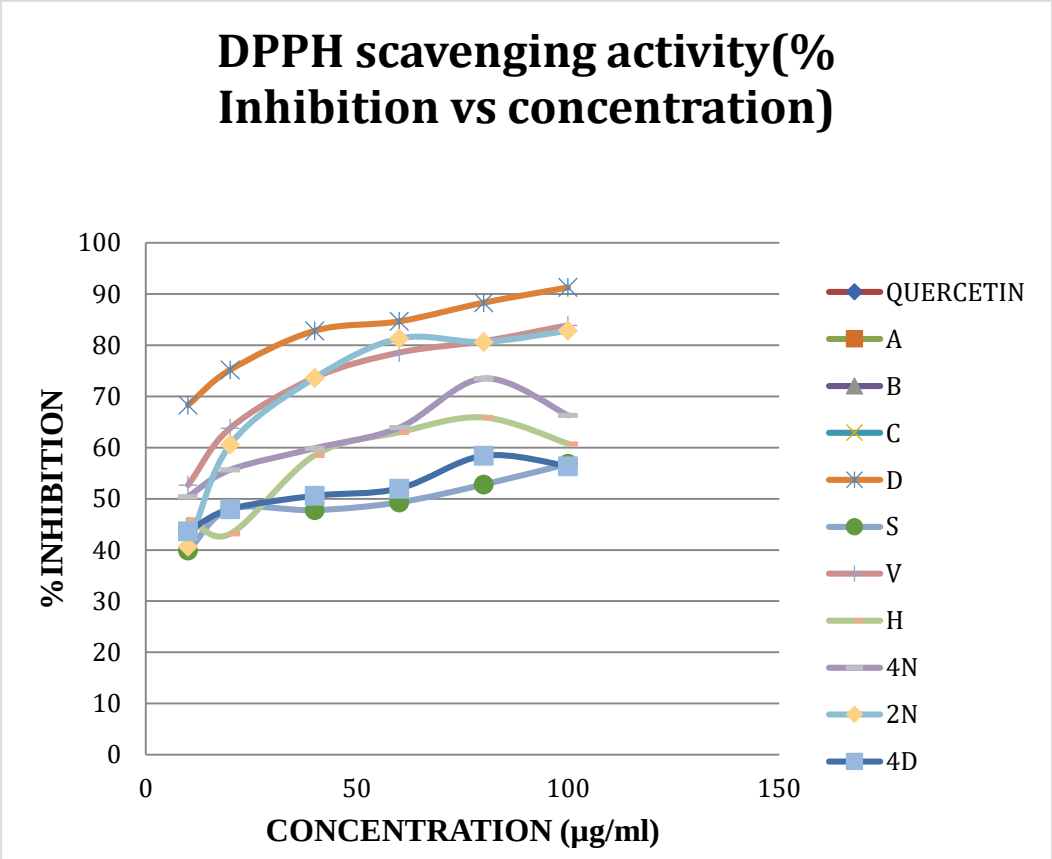

4.6.3 IC_{50} Values of compounds and standard.

Table 7: IC_{50} values of experimental compounds by DPPH free radical scavenging activity.

COMPOUND	IC_{50} VALUES.
A	98.13
B	70.29
C	87.67
D	54.76
S	87.98
V	59.60
H	82.31
4N	75.43
2N	60.35
4D	88.67
Quercetin	52.24

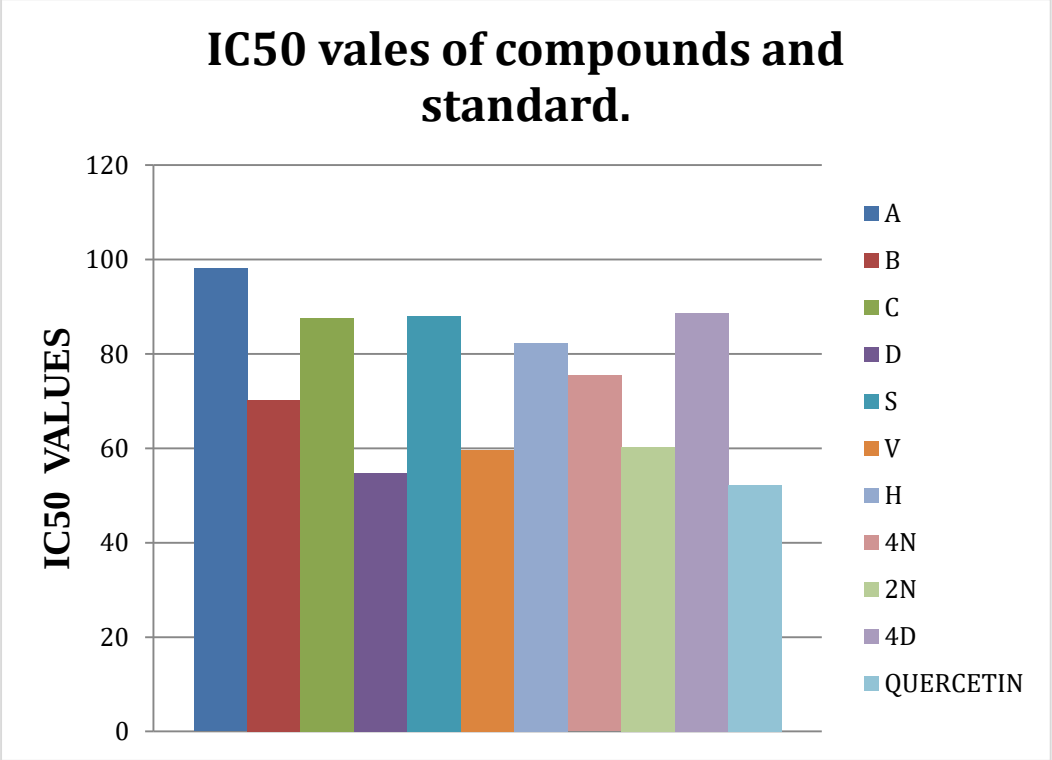

Figure 8: IC_{50} values (in µg/ml) of experimental compounds by DPPH free radical scavenging activity.

By comparing IC_{50} values of the compounds with standard used i.e Quercetin, it has been observed that compound V, D,2N shows moderate antioxidant activity compared to Quercetin.

DISCUSSION:

In recent years, there has been a significant increase in efforts to discover and develop newer anticancer and antioxidant drugs, primarily driven by the challenges posed by drug resistance in existing treatments. Several methods have been reported for synthesizing curcumin analogues, employing various boron catalysts. However, these methods have their limitations, such as the formation of side products when substituting at the C3 carbon, long reaction times, difficulties in chromatographic separation due to the formation of Schiff bases, and the use of costly catalysts. To overcome these limitations, we successfully carried out the synthesis of new curcumin analogues using a novel approach. We replaced boric oxide and boric anhydride with boron trifluoride etherate as the catalyst and optimized the reaction conditions. We carefully monitored and optimized parameters such as the number of reactant moles, catalyst concentration, reaction temperature, and solvent selection. This resulted in a time-saving and efficient reaction process, yielding clean and well-defined products. The synthesized compounds were characterized using physical constants and spectral studies, including IR and NMR analyses. Furthermore, their antioxidant activity was evaluated, with some compounds demonstrating moderate activity when compared to the antioxidant Quercetin. Notably, compounds V, D, and 2N exhibited moderate IC50 values in comparison to Quercetin. In addition to antioxidant activity, we also assessed the anticancer activity of these compounds against MCF7, K562, and HEPG2 cell lines. The results of these evaluations provide valuable insights into the potential anticancer properties of the synthesized compounds. Overall, our study successfully developed a newer synthetic approach for curcumin analogues, addressing the limitations associated with previous methods. The synthesized compounds were characterized and evaluated for their antioxidant and anticancer activities, showing promising results. These findings contribute to the ongoing quest for new and effective anticancer and antioxidant drugs, opening avenues for further research and exploration in the field of drug discovery.

CONCLUSION:

Curcumin and its analogues show great potential as future candidates for both anticancer and antioxidant therapies. With this in mind, we synthesized analogues of curcumin and aimed to improve the results by replacing the catalyst. In our study, we successfully developed Boron trifluoride etherate as a catalyst for the synthesis of 1,7-bis(4-hydroxy-3-methoxyphenyl)-1,6-heptadiene-3,5-dione substitutes. This new catalyst led to better yields and

reduced reaction times compared to other methods. We confirmed the formation of the compounds through various analyses such as IR, melting point, and 1HNMR. The synthesized compounds were then evaluated for their antioxidant and anticancer activity. Our findings indicate that these compounds exhibited significant cytotoxic activity against MCF7 and K562 cell lines, which correlated with their antioxidant properties. Some of the compounds displayed moderate activity. Notably, the compounds containing -OCH3, -OH, and NO2 groups showed activity similar to that of Adriamycin (Doxorubicin) on the MCF7 cell line. Additionally, the compound with -OCH3 functionality exhibited comparable activity to Adriamycin on the K562 cell line. This suggests that electron-dense groups in the compounds contribute to their activity against MCF7 cells. However, none of the compounds showed activity against the HEPG2 cell line, possibly due to the highly lipophilic nature of these cell lines. Among all the synthesized compounds, 1,7-bis(3,4-dimethoxyphenyl) hepta-1,6-diene-3,5-dione (D) demonstrated equivalent activity to Doxorubicin against both MCF7 and K562 cell lines. Based on these results, it can be concluded that 1,7-bis(3,4-dimethoxyphenyl) hepta-1,6-diene-3,5-dione (D) holds great potential as a new anticancer drug or as part of a drug combination to combat drug resistance in cancer treatment. This compound presents itself as a promising candidate for further exploration and development. This study contributes valuable data to the field of anticancer and antioxidant research, offering insights for the development of new drugs in these areas. While it is premature to definitively conclude the effectiveness of the studied compounds as anticancer and antioxidants, these findings provide a foundation for further investigation into potent drugs against cancer and oxidative stress.

References

1. Zugazagoitia, J., Guedes, C., Ponce, S., Ferrer, I., Molina-Pinelo, S. and Paz-Ares, L., 2016. Current challenges in cancer treatment. Clinical therapeutics, 38(7), pp.1551-1566.
2. Taplin, S.H., Anhang Price, R., Edwards, H.M., Foster, M.K., Breslau, E.S., Chollette, V., Prabhu Das, I., Clauser, S.B., Fennell, M.L. and Zapka, J., 2012. Introduction: understanding and influencing multilevel factors across the cancer care continuum. Journal of the National Cancer Institute Monographs, 2012(44), pp.2-10.
3. Shewach, D.S. and Kuchta, R.D., 2009. Introduction to cancer chemotherapeutics. Chemical reviews, 109(7), pp.2859-2861.
4. Taplin, S.H., Anhang Price, R., Edwards, H.M., Foster, M.K., Breslau, E.S., Chollette, V., Prabhu Das, I., Clauser, S.B., Fennell, M.L. and Zapka, J., 2012. Introduction: understanding and influencing multilevel factors across the cancer care continuum. Journal of the National Cancer Institute Monographs, 2012(44), pp.2-10.
5. Galon, J., Mlecnik, B., Bindea, G., Angell, H.K., Berger, A., Lagorce, C., Lugli, A., Zlobec, I., Hartmann, A., Bifulco, C. and Nagtegaal, I.D., 2014. Towards the introduction of the 'Immunoscore'in the classification of malignant tumours. The Journal of pathology, 232(2), pp.199-209.
6. Dickman, P.W. and Adami, H.O., 2006. Interpreting trends in cancer patient survival. Journal of internal medicine, 260(2), pp.103-117.
7. Dawood, S., Austin, L. and Cristofanilli, M., 2014. Cancer stem cells: implications for cancer therapy. Oncology (Williston Park), 28(12), pp.1101-7.
8. Curado, M.P., Edwards, B., Shin, H.R., Storm, H., Ferlay, J., Heanue, M. and Boyle, P., 2007. Cancer incidence in five continents, Volume IX. IARC Press, International Agency for Research on Cancer.
9. Howell, A., Anderson, A.S., Clarke, R.B., Duffy, S.W., Evans, D.G., Garcia-Closas, M., Gescher, A.J., Key, T.J., Saxton, J.M. and Harvie, M.N., 2014. Risk determination and prevention of breast cancer. Breast Cancer Research, 16(5), pp.1-19.
10. Crawford, E.D., 2003. Epidemiology of prostate cancer. Urology, 62(6), pp.3-12.
11. Tuveson, D. and Clevers, H., 2019. Cancer modeling meets human organoid technology. Science, 364(6444), pp.952-955.
12. Tomeh, M.A., Hadianamrei, R. and Zhao, X., 2019. A review of curcumin and its derivatives as anticancer agents. International journal of molecular sciences, 20(5), p.1033.
13. Aggarwal, B.B., Kumar, A. and Bharti, A.C., 2003. Anticancer potential of curcumin: preclinical and clinical studies. Anticancer research, 23(1/A), pp.363-398.
14. Kunnumakkara, A.B., Bordoloi, D., Harsha, C., Banik, K., Gupta, S.C. and Aggarwal, B.B., 2017. Curcumin mediates anticancer effects by modulating multiple cell signaling pathways. Clinical science, 131(15), pp.1781-1799.
15. Perrone, D., Ardito, F., Giannatempo, G., Dioguardi, M., Troiano, G., Lo Russo, L., De Lillo, A., Laino, L. and Lo Muzio, L., 2015. Biological and therapeutic activities, and

anticancer properties of curcumin. Experimental and therapeutic medicine, 10(5), pp.1615-1623.
16. Panda, A.K., Chakraborty, D., Sarkar, I., Khan, T. and Sa, G., 2017. New insights into therapeutic activity and anticancer properties of curcumin. Journal of experimental pharmacology, pp.31-45.
17. Vyas, A., Dandawate, P., Padhye, S., Ahmad, A. and Sarkar, F., 2013. Perspectives on new synthetic curcumin analogs and their potential anticancer properties. Current pharmaceutical design, 19(11), pp.2047-2069.
18. Allegra, A., Innao, V., Russo, S., Gerace, D., Alonci, A. and Musolino, C., 2017. Anticancer activity of curcumin and its analogues: preclinical and clinical studies. Cancer investigation, 35(1), pp.1-22.
19. Sun, A., Shoji, M., Lu, Y.J., Liotta, D.C. and Snyder, J.P., 2006. Synthesis of EF24− tripeptide chloromethyl ketone: a novel curcumin-related anticancer drug delivery system. Journal of medicinal chemistry, 49(11), pp.3153-3158.
20. Kuttan, R., Bhanumathy, P., Nirmala, K. and George, M.C., 1985. Potential anticancer activity of turmeric (Curcuma longa). Cancer letters, 29(2), pp.197-202.